Three-Dimensional Kneed Bipedal Walking: A Hybrid Geometric Approach

Aaron D. Ames, Ryan W. Sinnet, and Eric D.B. Wendel

Department of Mechanical Engineering
Texas A&M University, College Station, TX
aames@tamu.edu, {rsinnet,ericdbw}@neo.tamu.edu

Abstract. A 3D biped with knees and a hip is naturally modeled as a nontrivial hybrid system; impacts occur when the knee strikes and when the foot impacts the ground causing a switch in the dynamics governing the system. Through a variant of geometric reduction—termed *functional Routhian reduction*—we can reduce the dynamics on each domain of this hybrid system to obtain a planar equivalent biped. Using preexisting techniques for obtaining walking gaits for 2D bipeds, and utilizing the decoupling effect afforded by the reduction process, we design control strategies that result in stable walking gaits for the 3D biped. That is, the main result of this paper is a control law that results in 3D bipedal walking obtained through stable walking gaits for the equivalent 2D biped.

1 Introduction

Adding knees to a bipedal robot is important from both a practical and theoretical perspective: knees allow for an increase in energy efficiency and for the ability to navigate rough terrain more robustly. Yet adding knees significantly adds to the complexity of analyzing and controlling the biped [4], [13]. To see this, note that bipedal robots are naturally modeled as hybrid systems; when the foot impacts the ground, there is an instantaneous change in the velocity of the system. Adding locking knees to the robot results in an even more complex hybrid model since at knee lock there is another instantaneous change in the velocity of the system. Moreover, this necessarily results in two sets of dynamical equations: one where the knee is unlocked and one where the knee is locked. Kneed walking, therefore, provides significant novel challenges, especially when coupled with the desire for three-dimensional bipedal walking.

Three-dimensional (3D) bipedal walking provides interesting challenges not found in its two-dimensional (2D) counterpart. In this case one must not only achieve stable forward motion, but simultaneously stabilize the walker upright during this motion. In addition, while 2D bipedal walking has been well-studied (see [6], [7], [12], [18] and [14] to name a few), the results in 3D bipedal walking are relatively limited (see [5], [9] and [8] for some results in 3D walking) and there have yet to be results on obtaining walking for 3D bipedal robots with knee locking. Coupling the study of 3D bipeds with the study of locking knees,

R. Majumdar and P. Tabuada (Eds.): HSCC 2009, LNCS 5469, pp. 16–30, 2009.

therefore, forms a challenge that will test our understanding of the underlying mechanisms of walking.

Fundamental to understanding 3D walking—with or without knees—is understanding the interplay between the lateral and sagittal dynamics. That is, we must mathematically quantify how to "decouple" the dynamics of a 3D biped into its sagittal and lateral components; this is done by exploiting inherent symmetries in walkers through the use of geometric reduction. Specifically, we consider a form of geometric reduction termed *functional Routhian reduction* (first introduced in [3] and generalized in [2]). As with classical reduction, this form of reduction utilizes symmetries in a system, in the form of "cyclic" variables, to reduce the dimensionality of the system. Unlike classical reduction, this is done by setting the conserved quantities equal to an arbitrary function of the "cyclic" variables rather than a constant, i.e., there is a *functional conserved quantity*. This allows us to "control" the decoupling effect of geometric reduction through this function, a fact that will be instrumental in the construction of our control law.

The main result of this paper is a control law that results in stable walking for a 3D biped with knees and a hip, which is achieved by combining three control laws. The first control law affects the sagittal dynamics of the biped by shaping the potential energy so that the 2D biped, obtained by constraining the 3D biped to the sagittal plane, has stable walking gaits. The second control law shapes the total energy of the 3D biped so that functional Routhian reduction can be applied—the reduced system is exactly the 2D system after applying the first control law—thus decoupling the sagittal and lateral dynamics, while allowing us to affect the lateral dynamics through our specific choice of the functional conserved quantity, for *certain initial conditions*. Finally, the third control law stabilizes to the surface of initial conditions for which the decoupling afforded by the second control law is valid. We verify numerically that the combined control law results in stable walking, i.e., a locally exponentially stable periodic orbit.

2 Bipedal Model

Hybrid systems are systems that display both continuous and discrete behavior and so bipedal walkers are naturally modeled by systems of this form; the continuous component consists of the dynamics dictated by Lagrangians modeling mechanical systems in different domains, and the discrete component consists of the impact equations which instantaneously change the velocity of the system when the knees lock or when the foot contacts the ground. This section, therefore, introduces the basic terminology of hybrid systems and introduces the hybrid model of the biped considered in this paper.

Definition 1. *A* hybrid control system *is a tuple*

$$\mathscr{HC} = (\Gamma, D, U, G, R, FG),$$

where

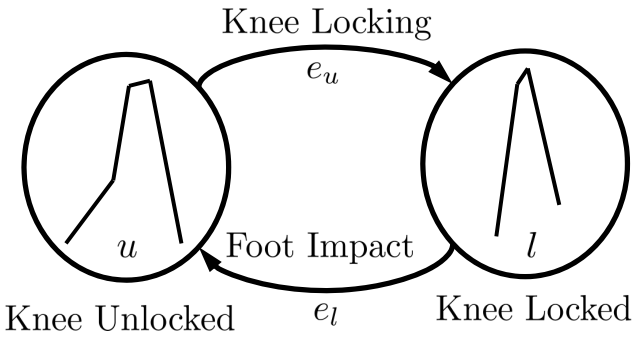

Fig. 1. A graphical representation of the domains of the hybrid control system $\mathscr{HC}_{3\mathrm{D}}$

- $\Gamma = (V, E)$ *is an oriented graph, i.e.,* V *and* E *are a set of vertices and edges, respectively, and there exists a source function* $\mathrm{sor} : E \to V$ *and a target function* $\mathrm{tar} : E \to V$ *which associates to an edge its source and target, respectively.*
- $D = \{D_v\}_{v \in V}$ *is a set of domains, where* $D_v \subseteq \mathbb{R}^{n_v}$ *is a smooth submanifold of* $\mathbb{R}^{n_v}$*,*
- $U = \{U_v\}_{v \in V}$*, where* $U_v \subset \mathbb{R}^{k_v}$ *is a set of admissible controls,*
- $G = \{G_e\}_{e \in E}$ *is a set of guards, where* $G_e \subseteq D_{\mathrm{sor}(e)}$*,*
- $R = \{R_e\}_{e \in E}$ *is a set of reset maps, where* $R_e : G_e \to D_{\mathrm{tar}(e)}$ *is a smooth map,*
- $FG = \{(f_v, g_v)\}_{v \in E}$*, where* (f_v, g_v) *is a control system on* D_v*, i.e.,* $\dot{x} = f_v(x) + g_v(x)u$ *for* $x \in D_v$ *and* $u \in U_v$*.*

A hybrid system $\mathscr{H} = (\Gamma, D, G, R, F)$ *is a hybrid control system with* $U = \{0\}$*, in which case* $F = \{f_v\}_{v \in E}$*.*

Solutions to hybrid systems, or *hybrid flows* or *hybrid executions*, are defined in the traditional manner (see [10]). A solution to a hybrid system is k-periodic if it returns to the same point after passing through the domain in which it is contained k times (in the process it may pass through an arbitrary number of other domains of the hybrid system). One can consider the local exponential stability of k-periodic solutions in the obvious way (see [2] for this definition in the case of a hybrid system with one domain). One can associate to a k-periodic solution of a hybrid system a Poincare map, and the stability of the k-periodic solution can be determined by considering the stability of the Poincare map. Finally, the stability can be determined numerically using approximations of the Jacobian of the Poincare map (see [14] and [15]). This is how we will determine that the periodic orbit for the 3D biped produced in this paper is stable.

3D biped model. The model of interest is a controlled bipedal robot with a hip, knees and splayed legs that walks on flat ground in three dimensions (see Figure 2), from which we will explicitly construct the hybrid control system:

$$\mathscr{HC}_{3\mathrm{D}} = (\Gamma_{3\mathrm{D}}, D_{3\mathrm{D}}, U_{3\mathrm{D}}, G_{3\mathrm{D}}, R_{3\mathrm{D}}, FG_{3\mathrm{D}}).$$

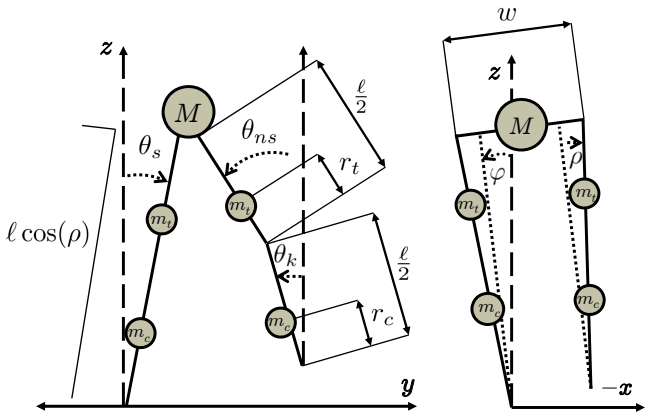

Fig. 2. The sagittal and lateral planes of a three-dimensional bipedal robot

In particular, $\Gamma_{3\mathrm{D}} = (\{u, l\}, \{e_u = (u, l), e_l = (l, u)\})$. That is, there are two domains u, l and two edges e_u, e_l (see Figure 1). In the first domain the biped's non-stance knee is unlocked and in the second domain the biped's knee is locked. Transitions occur from domain u to domain l when the knee locks, and from l to u when the foot strikes the ground. Note that the discrete structure of this model enforces temporal ordering to events (kneelock and footstrike) as motivated by the two-dimensional biped with knees considered in [4]. We will now construct the rest of the hybrid system $\mathscr{HC}_{3\mathrm{D}}$ beginning on the level of Lagrangians and constraint functions (see [1,2,3]).

Associated with each domain, there is a configuration space $Q_u^{3\mathrm{D}} = \mathbb{T}^3 \times \mathbb{S}^1$ and $Q_l^{3\mathrm{D}} = \mathbb{T}^2 \times \mathbb{S}^1$ associated with the knee being unlocked and locked, respectively. The coordinates on $Q_u^{3\mathrm{D}}$ are given by $q_u = (\theta_u^T, \varphi)^T$, with $\theta_u = (\theta_{\mathrm{s}}, \theta_{\mathrm{ns}}, \theta_{\mathrm{k}})^T$ the vector of sagittal-plane variables with the knee unlocked, where θ_{s} is the angle of the stance leg from vertical, θ_{ns} is the angle of the non-stance leg from vertical and θ_{k} is the angle of the knee from vertical (see Figure 2), and φ is the lean (or roll) from vertical. Similarly, the coordinates on $Q_l^{3\mathrm{D}}$ are given by $q_l = (\theta_l^T, \varphi)^T$, where $\theta_l = (\theta_{\mathrm{s}}, \theta_{\mathrm{ns}})^T$ is again the vector of sagittal-plane variables with the knee locked. Note that the hip width w, leg length ℓ, and leg splay angle ρ are held constant.

Each domain and guard are constructed from constraint functions. For the knee unlocked domain, the unilateral constraint is given by:

$$H_u^{3\mathrm{D}}(q_u) = \theta_{\mathrm{k}} - \theta_{\mathrm{ns}},$$

which is positive when the knee is unlocked and zero at kneestrike. For the knee locked domain, the unilateral constraint is given by:

$$H_l^{3\mathrm{D}}(q_l) = \ell\cos(\rho)\left(\cos(\theta_s) - \cos(\theta_{ns})\right)\cos(\varphi) + (w - 2\sin(\rho))\sin(\varphi),$$

which gives the height of the non-stance foot above the ground. Thus the domains for the hybrid system $D_{3\mathrm{D}} = \{D_u^{3\mathrm{D}}, D_l^{3\mathrm{D}}\}$ are obtained by requiring that the constraint functions be positive, i.e., for $i \in \{u, l\}$,

$$D_i^{3\mathrm{D}} = \left\{ \begin{pmatrix} q_i \\ \dot{q}_i \end{pmatrix} \in TQ_i^{3\mathrm{D}} : H_i^{3\mathrm{D}}(q_i) \geq 0 \right\}.$$

We put no restrictions on the set of admissible controls except that they can only directly affect the angular accelerations. Therefore, $U_{3\mathrm{D}} = \{U_u^{3\mathrm{D}}, U_l^{3\mathrm{D}}\}$ with $U_u^{3\mathrm{D}} = \mathbb{R}^4$ and $U_l^{3\mathrm{D}} = \mathbb{R}^3$.

The set of guards is given by $G_{3\mathrm{D}} = \{G_{e_u}^{3\mathrm{D}}, G_{e_l}^{3\mathrm{D}}\}$ where $G_{e_u}^{3\mathrm{D}}$ is the set of states where the leg is locking and $G_{e_l}^{3\mathrm{D}}$ is the set of states in which the height of the swing foot is zero and infinitesimally decreasing. That is, for $i \in \{u, l\}$,

$$G_{e_i}^{3\mathrm{D}} = \left\{ \begin{pmatrix} q_i \\ \dot{q}_i \end{pmatrix} \in TQ_i^{3\mathrm{D}} : H_i^{3\mathrm{D}}(q_i) = 0, \quad dH_i^{3\mathrm{D}}(q_i)\dot{q}_i < 0 \right\},$$

with $dH_i^{3\mathrm{D}}(q_i) = \left(\frac{\partial H_i^{3\mathrm{D}}}{\partial q_i}(q_i) \right)^T$.

The set of reset maps is given by $R_{3\mathrm{D}} = \{R_{e_u}^{3\mathrm{D}}, R_{e_l}^{3\mathrm{D}}\}$. The reset map $R_{e_u}^{3\mathrm{D}}$ is given by

$$R_{e_u}^{3\mathrm{D}}(q_u, \dot{q}_u) = \begin{pmatrix} q_l \\ P(q_u, \dot{q}_u)_1 \\ P(q_u, \dot{q}_u)_2 \\ P(q_u, \dot{q}_u)_4 \end{pmatrix}$$

where

$$P(q_u, \dot{q}_u) = \dot{q}_u - \frac{dH_u^{3\mathrm{D}}(q_u)\dot{q}_u}{dH_u^{3\mathrm{D}}(q_u) M_u^{3\mathrm{D}}(q_u)^{-1} dH_u^{3\mathrm{D}}(q_u)^T} M_u^{3\mathrm{D}}(q_u)^{-1} dH_u^{3\mathrm{D}}(q_u)^T$$

with $M_u^{3\mathrm{D}}(q_u)$ the inertia matrix given in (1). This reset map models a perfectly plastic impact at the knee.

The reset map $R_{e_l}^{3\mathrm{D}}$ similarly models a perfectly plastic impact at the foot. This is obtained through the same process outlined in [3] and [7] (see [4] for a nice explanation of the computation of the impact equations for a 2D kneed walker) but space constraints prevent the inclusion of this equation. Also, note that the signs of w and ρ are flipped during impact to model the change in stance leg.

Finally, the dynamics for $\mathscr{HC}_{3\mathrm{D}}$ are obtained from the Euler-Lagrange equations for the two mechanical systems in each domain. Specifically, the Lagrangian describing each system is given by, for $i \in \{u, l\}$,

$$L_i^{3\mathrm{D}}(q_i, \dot{q}_i) = \frac{1}{2}\dot{q}_i^T M_i^{3\mathrm{D}}(q_i)\dot{q}_i - V_i^{3\mathrm{D}}(q_i),$$

where $M_i^{3\mathrm{D}}(q_i)$ is the inertial matrix and $V_i^{3\mathrm{D}}(q_i)$ is the potential energy (these are large matrices and so space constraints prevent the inclusion of them in this paper), where $M_i^{3\mathrm{D}}(q_i)$ can be expressed in block matrix form as follows:

$$M_i^{3\mathrm{D}}(q_i) = \begin{pmatrix} M_i^{\theta}(\theta_i) & M_i^{\varphi,\theta}(\theta_i)^T \\ M_i^{\varphi,\theta}(\theta_i) & m_i^{\varphi}(\theta_i) \end{pmatrix}, \tag{1}$$

where $M_i^{3D}(q_i) \in \mathbb{R}^{n_i \times n_i}$, $M_i^{\theta}(\theta_i) \in \mathbb{R}^{(n_i-1)\times(n_i-1)}$, $M_i^{\varphi,\theta}(\theta_i) \in \mathbb{R}^{1\times(n_i-1)}$ and $m_i^{\varphi}(\theta_i) \in \mathbb{R}$ where $n_u = 4$ and $n_l = 3$. The reason for this block matrix representation will become clear when the control laws are introduced.

Using the controlled Euler-Lagrange equations, the dynamics for the walker are given by:

$$M_i^{3D}(q_i)\ddot{q}_i + C_i^{3D}(q_i, \dot{q}_i)\dot{q}_i + N_i^{3D}(q_i) = B_i^{3D} v_i,$$

where $v_i \in U_i^{3D}$, $C_i^{3D}(q_i, \dot{q}_i)$ is the Coriolis matrix, $N_i^{3D} = \frac{\partial V_i^{3D}}{\partial q_i}(q_i)$, and

$$B_l^{3D} = \begin{pmatrix} 1 & 0 & 0 \\ -1 & 1 & 0 \\ 0 & 0 & 1 \end{pmatrix}, \qquad B_u^{3D} = \begin{pmatrix} 1 & 0 & 0 & 0 \\ -1 & 1 & 0 & 0 \\ 0 & -1 & 1 & 0 \\ 0 & 0 & 0 & 1 \end{pmatrix},$$

which converts the torque from relative coordinates to absolute.

Thus for $FG_{3D} = \{FG_u^{3D}, FG_l^{3D}\}$, we have for $i \in \{u, l\}$

$$f_i^{3D}(q_i, \dot{q}_i) = \begin{pmatrix} \dot{q}_i \\ M_i^{3D}(q)^{-1}\left(-C_i^{3D}(q_i, \dot{q}_i)\dot{q}_i - N_i^{3D}(q_i)\right) \end{pmatrix},$$
$$g_i^{3D}(q_i, \dot{q}_i) = \begin{pmatrix} 0_{n_i \times n_i} \\ M_i^{3D}(q_i)^{-1} B_i^{3D} \end{pmatrix},$$

where $0_{n_i \times n_i}$ is a $n_i \times n_i$ matrix of zeros.

3 Control Law Construction

This section presents the control law for the 3D biped with a knee and hip, the construction of which is motivated by the control law for the 3D biped (without a knee) successfully utilized in [2]. In particular, the control law is obtained by combining three control laws on *each* domain, u and l, of the hybrid system. The first control law acts on the sagittal dynamics of the walker on each domain in a way analogous to the controlled symmetries control law used for 2D walkers, the second control law transforms the Lagrangians of the 3D walker into almost-cyclic Lagrangians so that we can utilize *functional Routhian reduction* (see [2]), and the third control law utilizes zero dynamics techniques to stabilize to the set of initial conditions where the decoupling effect afforded by functional Routhian reduction is in effect. The result of combining these control laws is a control law on each domain of the hybrid system that results in stable walking; the specific attributes of this walking will be discussed in the next section.

Reduced dynamics controller. The first control law affects the dynamics of the 3D biped's sagittal plane by shaping the potential energy of the Lagrangian describing these dynamics on each domain of the hybrid system as motivated by the controlled symmetries method of [17]. The end result is a hybrid system modeling the 2D dynamics of the biped that walks on flat ground.

We can view the 2D sagittal restriction of the 3D biped as a hybrid control system:

$$\mathscr{HC}_{2\mathrm{D}} = (\Gamma_{3\mathrm{D}}, D_{2\mathrm{D}}, U_{2\mathrm{D}}, G_{2\mathrm{D}}, R_{2\mathrm{D}}, FG_{2\mathrm{D}})$$

where $\Gamma_{2\mathrm{D}} = \Gamma_{3\mathrm{D}}$. To obtain this hybrid system we consider two configuration spaces $Q_u^{2\mathrm{D}} = \mathbb{T}^3$ and $Q_l^{2\mathrm{D}} = \mathbb{T}^2$ with coordinates $\theta_u = (\theta_{\mathrm{s}}, \theta_{\mathrm{ns}}, \theta_{\mathrm{k}})^T$ and $\theta_l = (\theta_{\mathrm{s}}, \theta_{\mathrm{ns}})^T$ and let

$$D_i^{2\mathrm{D}} = \left\{ \begin{pmatrix} \theta_i \\ \dot{\theta}_i \end{pmatrix} \in TQ_i^{2\mathrm{D}} : H_i^{2\mathrm{D}}(\theta_i) \geq 0 \right\},$$
$$G_{e_i}^{2\mathrm{D}} = \left\{ \begin{pmatrix} \theta_i \\ \dot{\theta}_i \end{pmatrix} \in TQ_i^{2\mathrm{D}} : H_i^{2\mathrm{D}}(\theta_i) = 0, dH_i^{2\mathrm{D}}(\theta_i)\dot{\theta}_i < 0 \right\},$$

for $i \in \{u, l\}$, with $H_i^{2\mathrm{D}}(\theta_i) = H_i^{3\mathrm{D}}(\theta_i, 0)$. We obtain the reset maps $R_{e_u}^{2\mathrm{D}}$ and $R_{e_l}^{2\mathrm{D}}$ by similarly projecting the reset maps to the $\varphi = 0$ subspace. For the set of admissible controls, we take $U_u^{2\mathrm{D}} = \mathbb{R}^3$ and $U_l^{2\mathrm{D}} = \mathbb{R}^2$. Finally, the dynamics $(f_i^{2\mathrm{D}}, g_i^{2\mathrm{D}})$, $i \in \{u, l\}$, are obtained from the Lagrangians given by:

$$L_i^{2\mathrm{D}}(\theta_i, \dot{\theta}_i) = \frac{1}{2}\dot{\theta}_i^T M_i^{2\mathrm{D}}(\theta_i)\dot{\theta}_i - V_i^{\theta}(\theta_i),$$

where $M_i^{2\mathrm{D}} = M_i^{\theta}$ as in (1) and $V_i^{2\mathrm{D}}(\theta_i) = V_i^{3\mathrm{D}}(\theta_i, 0)$, through the Euler Lagrange equations as was done in the 3D model, where in this case $B_u^{2\mathrm{D}}$ and $B_l^{2\mathrm{D}}$ are the 3×3 and 2×2 upper-left submatrices of $B_u^{3\mathrm{D}}$ and $B_l^{3\mathrm{D}}$, respectively.

The hybrid control system $\mathscr{HC}_{2\mathrm{D}}$ is similar, but not equivalent, to the typical 2D kneed walker (cf. [4]) (since the splayed legs affects the height of the planar robot) which motivates the control law to be introduced. That is, we utilize controlled symmetries of [17] by "rotating the world" via a group action in order to shape the potential energy of both $L_u^{2\mathrm{D}}$ and $L_l^{2\mathrm{D}}$ to obtain stable walking gaits on flat ground for $\mathscr{HC}_{2\mathrm{D}}$.

Consider the group action $\Psi_i : \mathbb{S}^1 \times Q_i^{2\mathrm{D}} \to Q_i^{2\mathrm{D}}$, $i \in \{u, l\}$, given by:

$$\Psi_l^{\gamma}(\theta_l) := \begin{pmatrix} \theta_{\mathrm{s}} + \gamma \\ \theta_{\mathrm{ns}} + \gamma \end{pmatrix}, \qquad \Psi_u^{\gamma}(\theta_u) := \begin{pmatrix} \theta_{\mathrm{s}} + \gamma \\ \theta_{\mathrm{ns}} + \gamma \\ \theta_{\mathrm{k}} + \gamma \end{pmatrix}$$

for slope angle $\gamma \in \mathbb{S}^1$. Using this, define the following two feedback control laws:

$$KR_i^{\gamma}(\theta_i) := (B_i^{2\mathrm{D}})^{-1} \left(\frac{\partial V_i^{2\mathrm{D}}}{\partial \theta_i}(\theta_i) - \frac{\partial V_i^{2\mathrm{D}}}{\partial \theta_i}(\Psi_i^{\gamma}(\theta_i)) \right), \tag{2}$$

for $i \in \{u, l\}$. Applying these control laws to the control systems $(f_i^{2\mathrm{D}}, g_i^{2\mathrm{D}})$ yields the dynamical systems:

$$f_i^{\gamma}(\theta_i, \dot{\theta}_i) := f_i^{2\mathrm{D}}(\theta_i, \dot{\theta}_i) + g_i^{2\mathrm{D}}(\theta_i, \dot{\theta}_i) KR_i^{\gamma}(\theta_i),$$

which are just the vector fields associated to the Lagrangians

$$L_i^{\gamma}(\theta_i, \dot{\theta}_i) = \frac{1}{2}\dot{\theta}_i^T M_i^{2\mathrm{D}}(\theta_i)\dot{\theta}_i - V_i^{2\mathrm{D}}(\Psi_i^{\gamma}(\theta_i)). \tag{3}$$

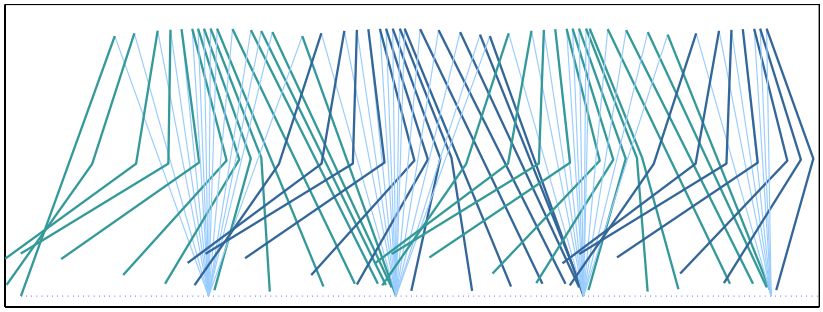

Fig. 3. A walking gait of the 2D biped obtained by restricting the 3D biped

We have thus defined a hybrid control system:

$$\mathscr{H}_{2\mathrm{D}}^{\gamma} := (\Gamma_{2\mathrm{D}}, D_{2\mathrm{D}}, G_{2\mathrm{D}}, R_{2\mathrm{D}}, F^{\gamma}),$$

where $F^{\gamma} = \{f_u^{\gamma}, f_l^{\gamma}\}$.

As with the typical kneed 2D biped, it can be verified that for certain γ, this hybrid system has a stable periodic orbit. An example of the 2D walking that is obtained for this 2D biped under this control law can be seen in Figure 3. Note that for this simulation, $\gamma = 0.0504$ (and the same model constants as used in Section 4) motivated by [4].

Lagrangian shaping controllers. The fundamental tool used in the construction of the second control law is *functional Routhian reduction* (see [2] for a complete discussion of this type of reduction). This is a variant of standard Routhian reduction [11], and allows one to reduce the dimensionality of dynamical systems obtained from "almost-cyclic" Lagrangians. Moreover, it differs from standard reduction techniques in that one can set the cyclic variables equal to a function, rather than a constant, thus affecting the behavior of these cyclic variables. This type of reduction is fundamental in the construction of our control law since the cyclic variable is the lean angle, so applying this reduction allows for the decomposition of the walker into its sagittal and lateral components.

More concretely, we introduce controllers to shape both the kinetic and potential energy of $L_i^{3\mathrm{D}}$, $i \in \{u, l\}$ so as to render them "almost-cyclic." This shaping is done so that the functional Routhians (the Lagrangians for the reduced systems) associated with these almost-cyclic Lagrangians are just the Lagrangians for the 2D kneed walker considered in the construction of the first control laws.

Consider the following almost-cyclic Lagrangians for $i \in \{u, l\}$:

$$L_i^{(\alpha,\gamma)}(\theta_i, \varphi, \dot{\theta}_i, \dot{\varphi}) = \frac{1}{2}\begin{pmatrix}\dot{\theta}_i^T & \dot{\varphi}\end{pmatrix} M_i^{\alpha}(\theta_i)\begin{pmatrix}\dot{\theta}_i \\ \dot{\varphi}\end{pmatrix} - W_i^{\alpha}(\theta_i, \varphi, \dot{\theta}_i) - V_i^{(\alpha,\gamma)}(\theta_i, \varphi),$$

where

$$M_i^{\alpha}(\theta_i) = \begin{pmatrix} M_i^{2\mathrm{D}}(\theta_i) + \frac{M_i^{\varphi,\theta}(\theta_i)^T M_i^{\varphi,\theta}(\theta_i)}{m_i^{\varphi}(\theta_i)} & M_i^{\varphi,\theta}(\theta_i)^T \\ M_i^{\varphi,\theta}(\theta_i) & m_i^{\varphi}(\theta_i) \end{pmatrix}$$

$$W_i^{\alpha}(\theta_i, \varphi, \dot{\theta}_i) = -\frac{\alpha\varphi}{m_i^{\varphi}(\theta_i)} M_i^{\varphi,\theta}(\theta_i)\dot{\theta}_i$$
$$V_i^{(\alpha,\gamma)}(\theta_i, \varphi) = V_i^{\text{2D}}(\Psi_i^{\gamma}(\theta_i)) - \frac{1}{2}\frac{\alpha^2\varphi^2}{m_i^{\varphi}(\theta_i)}$$

with $M_i^{\varphi,\theta}(\theta_i)$, $M_i^{\text{2D}}(\theta_i) = M_i^{\theta}(\theta_i)$, and $m_i^{\varphi}(\theta_i)$ as defined in (1)—the last two are positive definite since $M_i^{\text{3D}}(q_i) > 0$. Referring to [2], for these almost-cyclic Lagrangians, we have taken $\lambda(\varphi) = -\alpha\varphi$. It follows that the functional Routhians associated with these cyclic Lagrangians are L_i^{γ} as given in (3).

Now we can define two feedback control laws that transform L_i^{3D} to $L_i^{(\alpha,\gamma)}$. In particular, for $i \in \{u, l\}$, let

$$\begin{aligned} KS_i^{(\alpha,\gamma)}(q_i, \dot{q}_i) := (B_i^{\text{3D}})^{-1}(C_i^{\text{3D}}(q_i, \dot{q}_i)\dot{q}_i + N_i^{\text{3D}}(q_i) \\ + M_i^{\text{3D}}(q_i)M_i^{\alpha}(q_i)^{-1}(-C_i^{\alpha}(q_i, \dot{q}_i)\dot{q}_i - N_i^{(\alpha,\gamma)}(q_i))), \end{aligned} \tag{4}$$

where C_i^{α} is the shaped Coriolis matrix and $N_i^{(\alpha,\gamma)} = \frac{\partial V_i^{(\alpha,\gamma)}}{\partial q_i}$. Note that these control laws implicitly use the two first control laws. Applying these to the control systems $(f_i^{\text{3D}}, g_i^{\text{3D}})$ yields the dynamic systems:

$$f_i^{(\alpha,\gamma)}(q_i, \dot{q}_i) := f_i^{\text{3D}}(q_i, \dot{q}_i) + g_i^{\text{3D}}(q_i, \dot{q}_i)KS_i^{(\alpha,\gamma)}(q_i, \dot{q}_i), \tag{5}$$

which are just the vector fields associated to the Lagrangians $L_i^{(\alpha,\gamma)}$. Moreover we have the following relationship between the behavior of $f_i^{\alpha,\gamma}$ and f_i^{γ} on each domain of the hybrid system; this result follows directly from Theorem 1 in [2].

Theorem 1. *Let $i \in \{u, l\}$, then $(\theta_i(t), \varphi(t), \dot{\theta}_i(t), \dot{\varphi}(t))$ is a solution to the vector field $f_i^{(\alpha,\gamma)}$ on $[t_0, t_F]$ with*

$$\dot{\varphi}(t_0) = \frac{-1}{m_i^{\varphi}(\theta_i(t_0))}(\alpha\varphi(t_0) + M_i^{\varphi,\theta}(\theta_i(t_0))\dot{\theta}_i(t_0)), \tag{6}$$

if and only if $(\theta_i(t), \dot{\theta}_i(t))$ is a solution to the vector field f_i^{γ} and $(\varphi(t), \dot{\varphi}(t))$ satisfies:

$$\dot{\varphi}(t) = \frac{-1}{m_i^{\varphi}(\theta_i(t))}(\alpha\varphi(t) + M_i^{\varphi,\theta}(\theta_i(t))\dot{\theta}_i(t)). \tag{7}$$

This result implies that on each domain, for certain initial conditions, i.e., those satisfying (6), the dynamics of the biped can effectively be decoupled into the sagittal and lateral dynamics. Moreover, according to (7), the lateral dynamics must evolve in a very specific fashion. These fundamental points will allow us to use the walking gait for the 2D biped obtained by restricting the biped to obtain walking gaits for the 3D biped. But first, we must address how to handle situations where (6) is not satisfied.

Zero dynamics controller. The decoupling effect of Theorem 1 can only be enjoyed when (6) is satisfied; this set of initial conditions forms a hypersurface in each domain. Since most initial conditions will not satisfy this constraint, i.e., lie on this surface, we will use the classical method of output linearization in non-linear systems to stabilize to this hypersurface (see [16] for the continuous case and [7], [14] for the hybrid analogue).

Before introducing the third control law, we define a new hybrid control system that implicitly utilizes the first two control laws. Specifically, let

$$\mathscr{HC}_{3\mathrm{D}}^{(\alpha,\gamma)} = (\Gamma_{3\mathrm{D}}, D_{3\mathrm{D}}, \mathbb{R}, G_{3\mathrm{D}}, R_{3\mathrm{D}}, FG^{(\alpha,\gamma)})$$

where $\Gamma_{3\mathrm{D}}$, $D_{3\mathrm{D}}$, $G_{3\mathrm{D}}$ and $R_{3\mathrm{D}}$ are defined as for $\mathscr{HC}_{3\mathrm{D}}$ and

$$FG^{(\alpha,\gamma)} = \{(f_i^{(\alpha,\gamma)}, g_i^{(\alpha,\gamma)})\}_{i\in\{u,l\}}.$$

Each control system $(f_i^{(\alpha,\gamma)}, g_i^{(\alpha,\gamma)})$ is given by:

$$f_i^{(\alpha,\gamma)}(q_i,\dot{q}_i) + g_i^{(\alpha,\gamma)}(q_i,\dot{q}_i)v_i = f_i^{(\alpha,\gamma)}(q_i,\dot{q}_i) + g_i^{3\mathrm{D}}(q_i,\dot{q}_i)b_{n_i}v_i,$$

where $v_i \in \mathbb{R}$ and b_{n_i} is the n_i^{th} basis vector in $\mathbb{R}^{n_i}$ with $n_u = 4$ and $n_l = 3$ and $f_i^{(\alpha,\gamma)}$ as given in (5).

Motivated by our desire to satisfy (6), we define the following two functions for $i \in \{u, l\}$,

$$h_i(q_i,\dot{q}_i) := \dot{\varphi} + \frac{1}{m_i^{\varphi}(\theta_i)}(\alpha\varphi + M_i^{\varphi,\theta}(\theta_i)\dot{\theta}_i).$$

The main idea in the construction of the third control law is that we would like to drive $h_i(q_i,\dot{q}_i)$ to zero, i.e., we would like to drive the system to the surface

$$\mathcal{Z}_i = \left\{ \begin{pmatrix} q_i \\ \dot{q}_i \end{pmatrix} \in TQ_i^{3\mathrm{D}} : h_i(q_i,\dot{q}_i) = 0 \right\}.$$

With this in mind, and motivated by the standard method for driving an output function to zero in a nonlinear control system, we define the following feedback control laws:

$$v_i = KZ_i^{(\epsilon,\alpha,\gamma)}(q_i,\dot{q}_i) := \frac{-1}{L_{g_i^{(\alpha,\gamma)}}h_i(q_i,\dot{q}_i)}\left(L_{f_i^{(\alpha,\gamma)}}h_i(q_i,\dot{q}_i) + \frac{1}{\epsilon}h_i(q_i,\dot{q}_i)\right),$$

where $L_{g_i^{(\alpha,\gamma)}}h_i$ is the Lie derivative of h_i with respect to $g_i^{(\alpha,\gamma)}$, $L_{f_i^{(\alpha,\gamma)}}h_i$ is the Lie derivative of h_i with respect to $f_i^{(\alpha,\gamma)}$ and $KZ_i^{(\epsilon,\alpha,\gamma)}$ is well-defined since $L_{g_i^{(\alpha,\gamma)}}h_i(q_i,\dot{q}_i) \neq 0$. Note that under these control laws, each h_i will decay exponentially when the solution is in domain i since its evolution will be governed by the differential equation:

$$\dot{h}_i = -\frac{1}{\epsilon}h_i.$$

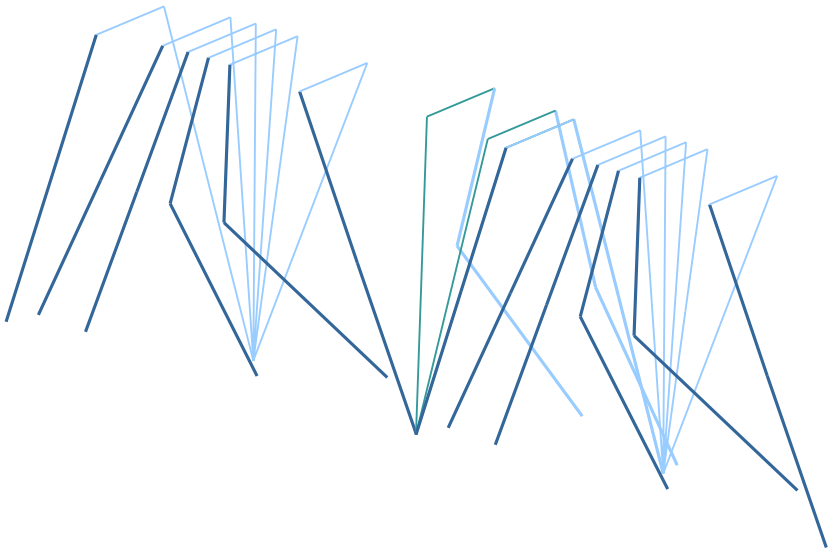

Fig. 4. A walking gait for the 3D biped

Utilizing the feedback control law $KZ_i^{(\epsilon,\alpha,\gamma)}$, we obtain a new hybrid system:

$$\mathscr{H}_{3D}^{(\epsilon,\alpha,\gamma)} := (\Gamma_{3D}, D_{3D}, G_{3D}, R_{3D}, F^{(\epsilon,\alpha,\gamma)}),$$

where $F^{(\epsilon,\alpha,\gamma)} = \{f_i^{(\epsilon,\alpha,\gamma)}\}_{i\in\{u,l\}}$ with

$$f_i^{(\epsilon,\alpha,\gamma)}(q_i,\dot{q}_i) := f_i^{(\alpha,\gamma)}(q_i,\dot{q}_i) + g_i^{(\alpha,\gamma)}(q_i,\dot{q}_i)KZ_i^{(\epsilon,\alpha,\gamma)}(q_i,\dot{q}_i).$$

Note that ϵ, α and γ can be thought of as control gains, as long as they are chosen so that $\epsilon > 0$, $\alpha > 0$, and γ such that $\mathscr{H}_{2D}^{\gamma}$ has a stable periodic orbit. We now proceed to examine the behavior of $\mathscr{H}_{3D}^{(\epsilon,\alpha,\gamma)}$.

4 Simulation Results

In this section we present simulation results supporting our claim that $\mathscr{H}_{3D}^{(\epsilon,\alpha,\gamma)}$ has a stable periodic orbit, i.e., that we obtain stable walking for the 3D biped.

We first choose model parameters $m_c = 0.05$kg, $m_t = 0.5$kg, $M_h = 0.5$kg, $\rho = 0.0188$rad, $w = 10$cm, $\ell = 1$m, $r_c = 0.372$m, $r_t = 0.175$m, $\gamma = 0.0504$rad, $\epsilon = \frac{1}{5}$, and $\alpha = 10$. The walking gait and stable limit cycle for our model with initial condition

$$x_0 = \big(0.000628 \quad 0.236309 \quad 0.236309 \quad -0.238929 \quad -0.238929$$
$$0.016716 \quad 1.513716 \quad 1.513716 \quad 1.590103 \quad 1.590103\big)^T$$

and these parameters is shown in Figure 4, 5 and 6, respectively. Note that each jump in the phase portraits shown corresponds to a jump from one vertex in

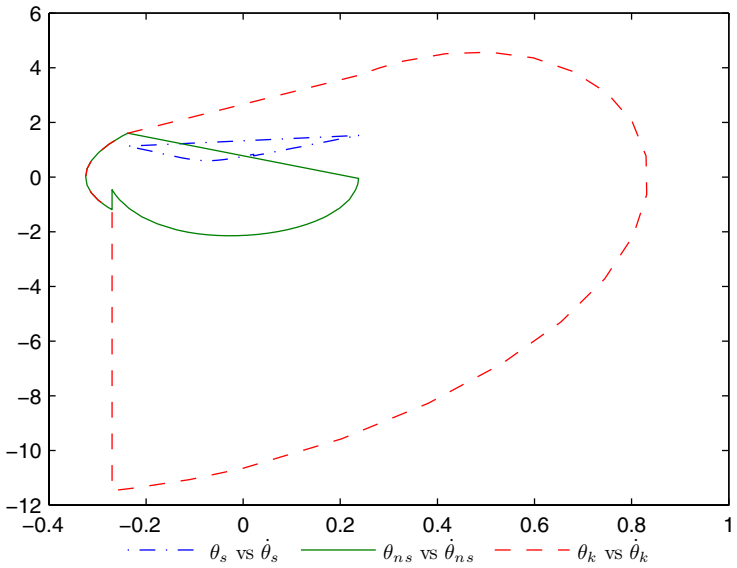

Fig. 5. A stable limit cycle of the 3D biped (top)

the graph Γ_{3D} to another and that, by inspection, the system appears to have a stable 2-periodic limit cycle.

We show that this limit cycle is (locally) exponentially stable by verifying that the eigenvalues of the linearized Poincare map at a fixed point of the limit cycle all have magnitude less than one [15]. Since our hybrid system consists of multiple domains we choose a fixed point right before footstrike, run the model forward two strides, and obtain five stable eigenvalues from the Jacobian of the Poincare map. The linearized Poincare map will always yield $n-1$ eigenvalues, where n is the dimension of the configuration space where the Poincare section of the Poincare map is located, since the Poincare section is by definition taken to be an $n-1$ dimensional hypersurface. Since our fixed point is in the knee-locked domain, our configuration space is Q_l^{3D}, of dimension 6. Thus, the 5 eigenvalues are $0.060149 \pm 0.593669i$, 0.000010, 0.004772 and 0.029407. The fact that these eigenvalues have magnitude much less than 1 suggests that the periodic orbit is both stable and that our third control law is effective at rejecting perturbations that might prevent the system from reaching a stable limit cycle.

The zero dynamics controller ensures that during the continuous evolution of the biped, solutions will converge exponentially to the surface $\mathcal{Z}_i$ where the sagittal and lateral dynamics are decoupled. What is interesting is that after each kneestrike or footstrike, the dynamics are thrown off the surface $\mathcal{Z}_i$ whereafter the zero dynamics controller again drives the system to the surface (this behavior can be seen in Figure 7). This could theoretically destroy the stability of walking in the sagittal plane, but fortunately does not due to two main facts: the perturbations away from the surface $\mathcal{Z}_i$ are not large, and the zero dynamics

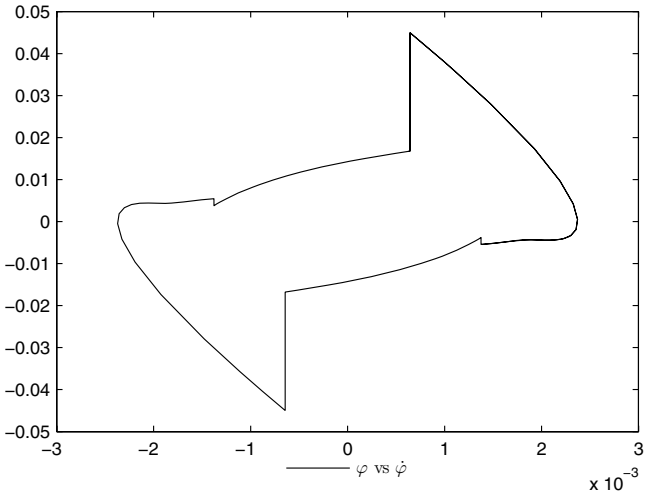

Fig. 6. A zoomed view of the lateral-plane (φ,$\dot{\varphi}$) limit cycle (bottom)

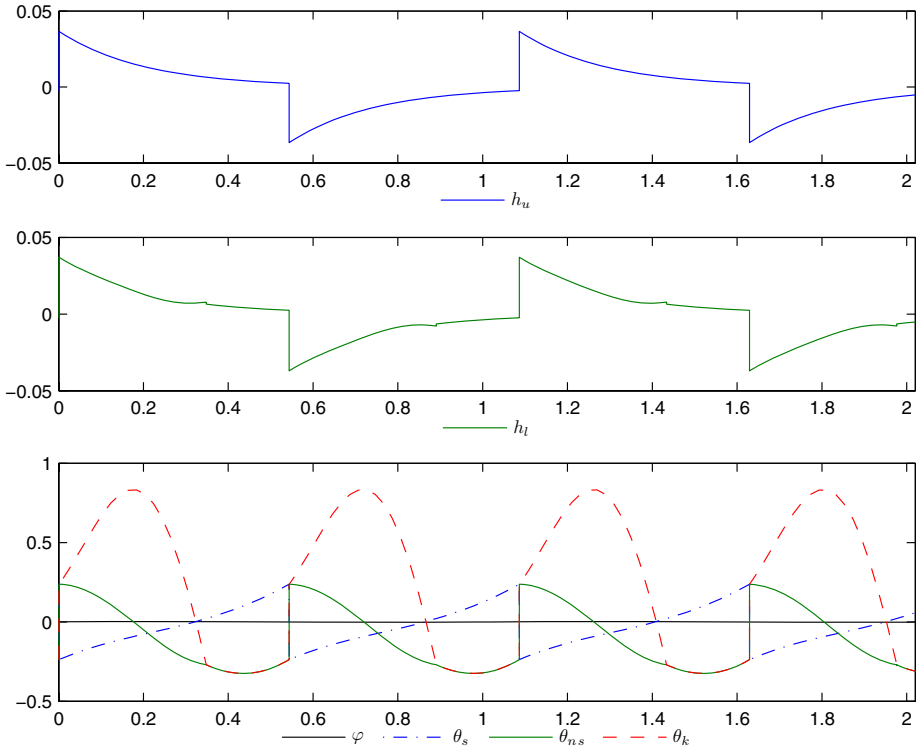

Fig. 7. The evolution of h_u and h_l for a walking gait of the 3D biped (top) and angles over time for the walking gait of the 3D biped (bottom)

brings the system close to the surface very quickly (exponentially fast) where again the decoupling effects are enjoyed. As a final note, the functions h_u and h_l will only decay exponentially when the solution is in domain u and l, respectively. This can be seen in the plot of h_l, where this function does not decay exponentially when the knee is unlocked, but does after kneestrike which occurs at the smaller jumps in the function.

The results of our simulation also indicate that we are able to obtain very natural walking using our three control laws. Looking at the time evolution of the knee angle θ_k in Figure 7, we see that in the knee-unlocked domain the leg swings naturally due to the passive dynamics, and then locks briefly before footstrike. It was shown in [2] that the natural side-to-side swaying, evident in the phase portrait of φ in Figure 6, is induced by the functional Routhian reduction used in the second control law. When the third control law brings the system close to the surface $\mathcal{Z}_i$, the phase portraits of the sagittal dynamics appear very similar to those of the 2D biped. As a result the stance and non-stance angles evolve like the 2D biped. In other words we have obtained stable, energy-efficient and natural walking gaits by virtue of the decoupling of the sagittal and lateral dynamics.

5 Conclusion

This paper presented a hybrid control law yielding stable walking for a three-dimensional biped with a hip and knees; while the result of this control law was natural-looking walking, indicating that it captures the natural dynamics of walking, there are numerous future research questions that result from this work. First, while the stability of the walking gait was verified numerically, the question is: can similar results be proven analytically? More importantly, in order to obtain these results, it was necessary to assume full actuation; since more complex walking involves phases of underactuation, dealing with underactuation in the context of the control scheme outlined here presents very interesting challenges. Finally, considering more complex bipedal robots is of fundamental importance, e.g., bipeds with feet. In considering these models, the corresponding hybrid systems will become increasingly complex with many more discrete domains and transitions between them. The final goal is to apply the general control strategy presented here to these more complex models in order to design bipedal walkers that display human looking walking.

Acknowledgments

The authors would like to thank Bobby Gregg and Mark Spong for their assistance in establishing results that lead to this paper. They would also like to thank Jessy Grizzle for many enlightening discussions on bipedal walking.

References

1. Ames, A.D., Gregg, R.D.: Stably extending two-dimensional bipedal walking to three dimensions. In: 26th American Control Conference, New York, NY (2007)
2. Ames, A.D., Gregg, R.D., Spong, M.W.: A geometric approach to three-dimensional hipped bipedal robotic walking. In: 45th Conference on Decision and Control, San Diago, CA (2007)
3. Ames, A.D., Gregg, R.D., Wendel, E.D.B., Sastry, S.: Towards the geometric reduction of controlled three-dimensional robotic bipedal walkers. In: 3rd Workshop on Lagrangian and Hamiltonian Methods for Nonlinear Control (LHMNLC 2006), Nagoya, Japan (2006)
4. Hsu Chen, V.F.: Passive dynamic walking with knees: A point foot model. Master's thesis, MIT (2007)
5. Collins, S.H., Wisse, M., Ruina, A.: A 3-d passive dynamic walking robot with two legs and knees. International Journal of Robotics Research 20, 607–615 (2001)
6. Goswami, A., Thuilot, B., Espiau, B.: Compass-like biped robot part I: Stability and bifurcation of passive gaits. Rapport de recherche de l'INRIA (1996)
7. Grizzle, J.W., Abba, G., Plestan, F.: Asymptotically stable walking for biped robots: Analysis via systems with impulse effects. IEEE Transactions on Automatic Control 46(1), 51–64 (2001)
8. Guobiao, S., Zefran, M.: Underactuated dynamic three-dimensional bipedal walking. In: Proceedings 2006 IEEE International Conference on Robotics and Automation, 2006. ICRA 2006, pp. 854–859 (2006)
9. Kuo, A.D.: Stabilization of lateral motion in passive dynamic walking. International Journal of Robotics Research 18(9), 917–930 (1999)
10. Lygeros, J., Johansson, K.H., Simic, S., Zhang, J., Sastry, S.: Dynamical properties of hybrid automata. IEEE Transactions on Automatic Control 48, 2–17 (2003)
11. Marsden, J.E., Ratiu, T.S.: Introduction to Mechanics and Symmetry. Texts in Applied Mathematics, vol. 17. Springer, Heidelberg (1999)
12. McGeer, T.: Passive dynamic walking. International Journal of Robotics Research 9(2), 62–82 (1990)
13. McGeer, T.: Passive walking with knees. In: IEEE International Conference on Robotics and Automation, Cincinnati, OH (1990)
14. Morris, B., Grizzle, J.W.: A restricted Poincaré map for determining exponentially stable periodic orbits in systems with impulse effects: Application to bipedal robots. In: 44th IEEE Conference on Decision and Control and European Control Conference, Seville, Spain (2005)
15. Parker, T.S., Chua, L.O.: Practical numerical algorithms for chaotic systems. Springer, New York (1989)
16. Sastry, S.: Nonlinear Systems: Analysis, Stability and Control. Springer, Heidelberg (1999)
17. Spong, M.W., Bullo, F.: Controlled symmetries and passive walking. IEEE Transactions on Automatic Control 50(7), 1025–1031 (2005)
18. Westervelt, E.R., Grizzle, J.W., Chevallereau, C., Choi, J.H., Morris, B.: Feedback Control of Dynamic Bipedal Robot Locomotion. Taylor & Francis/CRC (2007)